PROCEEDINGS OF SCIENCE

Hadronic model-independent method for determining cosmic-ray composition: Application to KASCADE data

N. Arsene[a,*]

[a] *Institute for Space Sciences - Subsidiary of INFLPR,*
P.O.Box MG-23, Ro 077125 Bucharest-Magurele, Romania

E-mail: nicusor.arsene@spacescience.ro

In this contribution, we present the results of the investigation into the utility of the *LCm* parameter as a discriminator for the mass composition of cosmic radiation recorded in experiments employing a relatively compact array of detectors. Based on the entire simulation/reconstruction chain of extensive air showers in the KASCADE experiment, we found that this *LCm* parameter is independent of the employed hadronic interaction models: QGSjet-II-04, EPOS-LHC, and SIBYLL 2.3d.

By reconstructing the experimental distributions of *LCm* from the measured data of the KASCADE experiment, we extracted the mass composition based on this parameter using Monte Carlo predictions for five primary species (p, He, C, Si, and Fe) in the energy range $\lg(E/\mathrm{eV}) = [15.0 - 16.0]$. The obtained results are highly consistent with those previously obtained by the KASCADE and IceTop Collaborations. Furthermore, the evolution of the individual fraction of particle types with primary energy is in excellent agreement with various astrophysical models that explain the *knee* as an effect of the acceleration and propagation of cosmic rays within the Galaxy.

38th International Cosmic Ray Conference (ICRC2023)
26 July - 3 August, 2023
Nagoya, Japan

*Speaker

PoS(ICRC2023)484

1. Introduction

For a better understanding of the mechanisms of production and acceleration of cosmic rays, and to be able to explain more precisely the main features in the energy spectrum (the *knee* at $E \sim 4 \times 10^{15}$ eV [15], the *second knee* at $E \sim 8 \times 10^{16}$ eV [2–4] and the *ankle* at $E \sim 5 \times 10^{18}$ eV [5, 6]), it is absolutely necessary to have a clearer picture of the mass composition of these primary cosmic rays across the entire energy spectrum.

A major interest has shifted towards the energy range around the *knee* due to recent highly significant discoveries regarding the detection of diffuse gamma rays from the Galactic disk with energies from hundreds of TeV up to 1.4 PeV [7, 8] which could lead to the discovery of the so-called PeVatrons within our Galaxy.

Given these recent important discoveries, a novel method for discriminating between gamma and hadron events has been developed in the context of experiments dedicated to studying cosmic and gamma rays, employing a relatively compact array of detectors [9–12]. This method introduces the LCm parameter, which exploits the non-uniformity in detector signals at a specific distance from the shower axis, induced by the presence of hadronic sub-showers generated during the development of extensive air showers.

Using the KASCADE data and simulations, we have shown that the LCm parameter can serve as an excellent discriminator in mass composition studies. Its major advantage lies in being independent of the hadronic interaction model considered in the simulation process of extensive air showers.

2. The LCm observable from MC simulations and KASCADE data

The stochastic nature of extensive air showers (EAS) development in Earth's atmosphere leads to uneven particle distributions at ground level. In vertical showers, one would expect consistent secondary particle densities at a fixed distance from the shower core. However, if we neglect the influence of the geomagnetic field, the presence of hadronic sub-showers can distort this expected symmetry. At comparable energies, a gamma-induced shower typically exhibits a simpler pattern of particle densities on the ground compared to a proton-induced shower. This is because gamma showers are predominantly governed by electromagnetic interactions. In the same context, we anticipate more pronounced fluctuations in the azimuthal signal in proton-induced showers compared to iron-induced showers, attributable to the greater variability in primary interaction heights within the atmosphere. The parameter $LCm = \log(C_k)$ was introduced to quantify this non-uniformity with the aim of discriminating between gamma and hadron-induced showers [9]:

$$C_k = \frac{2}{n_k(n_k-1)} \frac{1}{\langle S_k \rangle} \sum_{i=1}^{n_k-1} \sum_{j=i+1}^{n_k} (S_{ik} - S_{jk})^2, \tag{1}$$

where n_k denotes the number of detectors in ring k, $\langle S_k \rangle$ represents the mean signal recorded in the detectors of ring k, and S_{ik} and S_{jk} denote the signals in detectors i and j of ring k, the term $\frac{2}{n_k(n_k-1)}$ incorporates the inverse of the number of two-combinations for n_k detectors, denoted as $\binom{n_k}{2}$.

In this study, we reconstruct the *LCm* parameter for both data and simulations within the energy range $\lg(E/\mathrm{eV}) = [15.0 - 16.0]$, divided into intervals of $\lg(E/\mathrm{eV}) = 0.2$. This analysis is performed while considering the radial range $r_k = [100 - 110]$ m.

The simulation and reconstruction chain of extensive air showers (EAS) through the detector array of the KASCADE experiment was based on CORSIKA → CRES package based on GEANT3 → KRETA package (for reconstructing important cascade parameters) [13]. Three hadronic interaction models at high energies were considered: EPOS-LHC, QGSjet-II-04, and SIBYLL 2.3d, and FLUKA for low energies ($E_{\mathrm{lab}} < 200$ GeV). Simulations encompassed five primary particle species (p, He, C, Si, and Fe) within the energy range $\lg(E/\mathrm{eV}) = [15.0 - 16.0]$, with 0.2 intervals and an energy spectral index $\gamma = -2.7$. The zenith angles of the shower axis were isotropically sampled from the range $\theta = [0^\circ - 20^\circ]$ and the azimuthal distribution was uniformly sampled in the range $\phi = [0^\circ - 360^\circ]$. It is important to mention that the main parameters reconstructed from experimental data (primary energy, number of muons, number of electrons, zenith and azimuth angles of the cascade axis, etc.) were obtained using the same procedures as in the case of simulations, using the KRETA package.

For every primary particle species, hadronic interaction model, and energy range, we construct *LCm* distributions using Equation 1. Here, the signal S_i denotes the energy deposited by the electromagnetic component in the i-th e/γ-detector within the radial interval $r_k = [100 - 110]$ m around the shower core position. This parameter is independently measured by the muonic and hadronic energy deposited in KASCADE detectors. In this analysis, we used only the signal induced by the electromagnetic component because a significant portion of the muon detector grid is unavailable. If we had used an incomplete muon grid, it could have introduced an artificial variation in the azimuthal distribution of the signal in the detectors.

In Figure 1, we reconstructed from simulations the *LCm* distributions for showers induced by protons and Fe nuclei, considering the energy intervals $\lg(E/\mathrm{eV}) = [15.4 - 15.6]$ and $\lg(E/\mathrm{eV}) = [15.8 - 16.0]$, based on the three hadronic interaction models. Below each plot, we calculated the ratio of the distributions to emphasize that this *LCm* parameter is, within the available statistics, nearly independent of the used hadronic interaction model. We obtained the same level of agreement for the simulated intermediate elements (He, C, and Si).

The experimental *LCm* distributions obtained from the measurements at the KASCADE experiment are represented in Figure 2, divided into five energy intervals of 0.2 in the range $\lg(E/\mathrm{eV}) = [15.0 - 16.0]$. We considered only the events that survived the quality cuts recommended by the KASCADE collaboration [13].

3. Mass composition around the *knee*

To conduct a mass composition analysis by fitting the experimental data recorded in the KASCADE experiment with Monte Carlo (MC) templates obtained from simulations, we assessed the systematic uncertainties arising from the primary energy reconstruction and dependencies on MC mismodeling. Based on simulations, we obtained the systematic uncertainty in primary energy reconstruction and found it to vary between 20%-29%. Consequently, we were able to correct the bin-to-bin migration effect in the experimental *LCm* distributions. More details regarding the sensitivity, bias, and systematic errors of the method due to MC mismodeling can be found in [14].

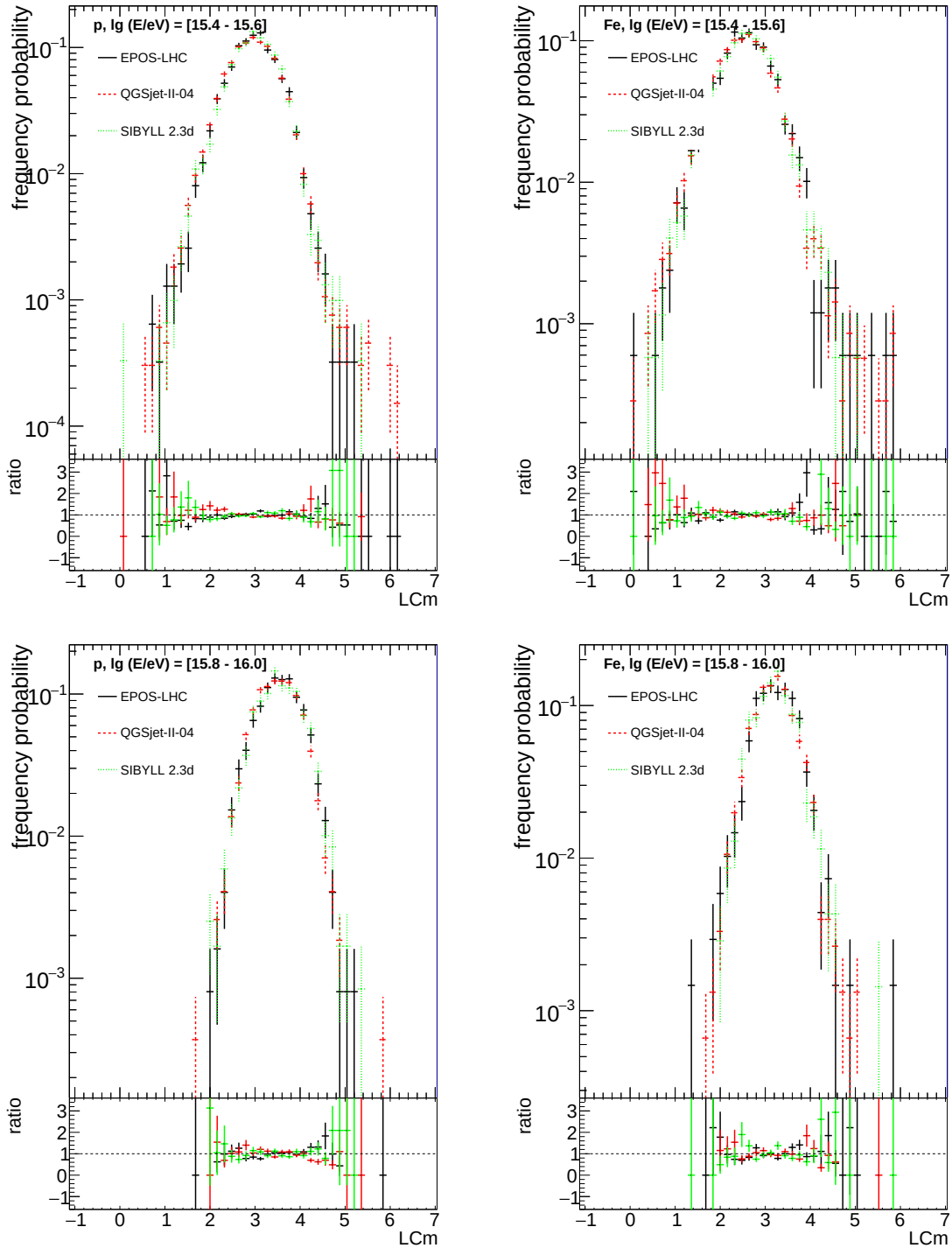

Figure 1: The *LCm* distributions for proton *(left)* and Fe *(right)* in the energy interval $\lg(E/\mathrm{eV})$ = [15.4 - 15.6] *(top)* and $\lg(E/\mathrm{eV})$ = [15.8 - 16.0] as predicted by all three hadronic interaction models considered in this work. The ratio of each pair of two distributions is displayed at the bottom of each plot.

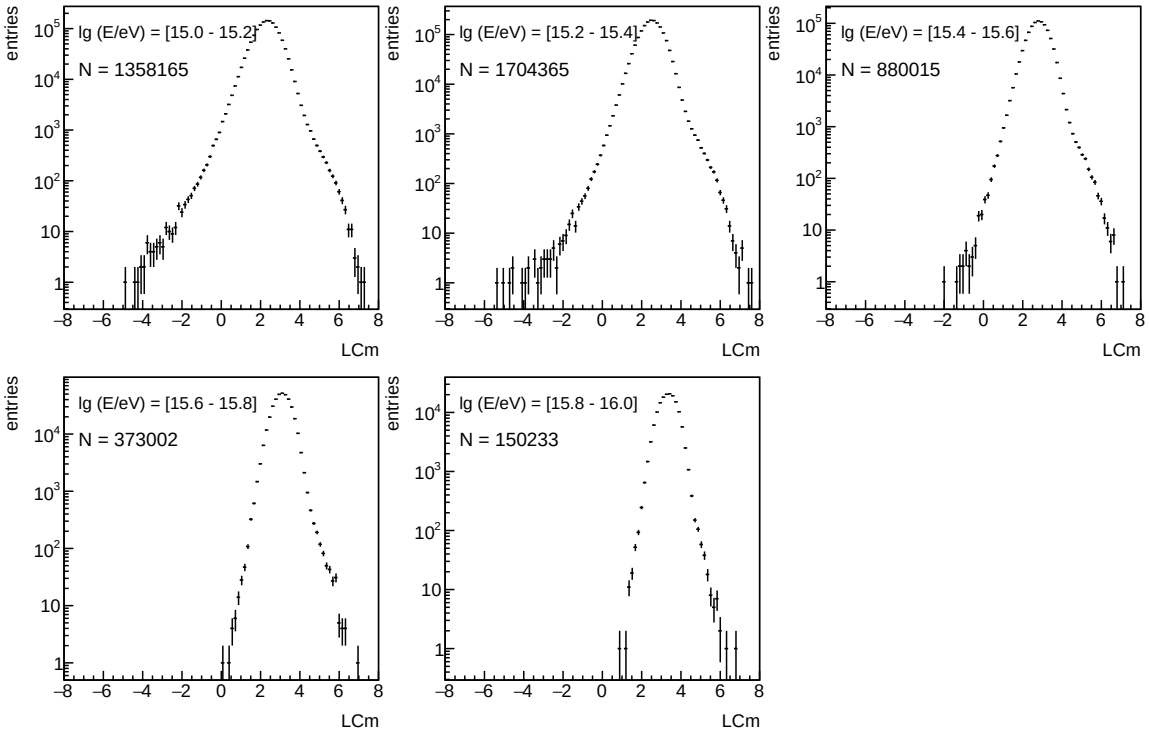

Figure 2: The *LCm* distributions reconstructed from KASCADE data in each energy interval in the range $\lg(E/\mathrm{eV}) = [15.0 - 16.0]$. The number of events N that survived all applied cuts is indicated on each plot. Figure taken from [14].

In this analysis, we employed KASCADE data to generate experimental *LCm* distributions, which were subsequently compared to Monte Carlo (MC) predictions for five primary species (p, He, C, Si, and Fe) utilizing three distinct hadronic interaction models (QGSjet-II-04, EPOS-LHC, and SIBYLL 2.3d). We utilized a Chi-Square minimization approach to fit the experimental distributions, and parameter errors were computed using the Minos technique.

The evolution of the abundance of each individual species as a function of energy obtained through this method is depicted in Figure 3. From the *top* graphs, it is evident that the mass composition of cosmic radiation obtained based on this parameter *LCm* practically does not depend on the considered hadronic interaction model, within the limits of statistical and systematic uncertainties. From the *middle* graphs, we observe that the results obtained in this analysis are in excellent agreement with results obtained through other complementary techniques by the KASCADE [15] and IceTop [16] collaborations. In the *bottom* plots of Figure 3, we demonstrated that the results obtained through this method support multiple astrophysical models explaining the *knee* feature in the energy spectrum as a consequence of the acceleration and propagation of cosmic rays within the Galaxy.

4. Conclusions

In this presentation, we summarized the results regarding the mass composition of cosmic radiation inferred based on the *LCm* parameter using the data and simulations from the KASCADE

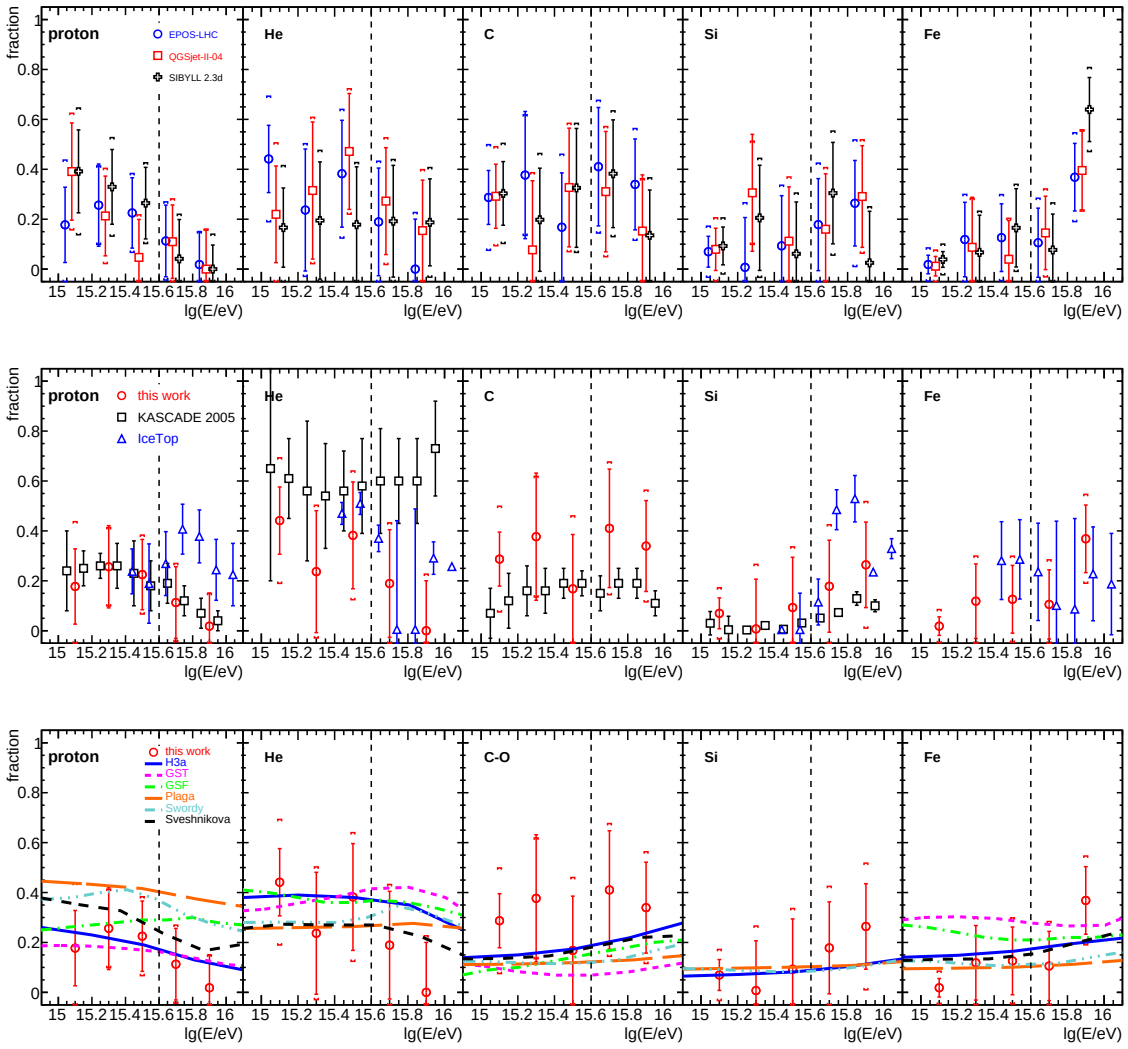

Figure 3: The evolution of individual fractions of nuclei (p, He, C, Si and Fe) as a function of primary energy (see text). The *(bottom)* plots represent the results obtained with QGSjet-II-04 model in comparison with predictions of different astrophysical models: H3a [17], GST [18], GSF [19], Plaga [20], Swordy [21] and Sveshnikova [22]. Figures taken from [14].

experiment. Some of these results have been further detailed in [14]. The main advantage of using this observable, LCm, is that it does not depend on the hadronic interaction model used in the extensive air shower simulation process. The mass composition as a function of energy obtained in this study aligns surprisingly well with prior findings reported by the KASCADE and IceTop experiments. Additionally, it can accommodate various astrophysical models attempting to explain the appearance of the *knee* in the energy spectrum.

Acknowledgments

This research was supported by the Romanian Ministry of Research, Innovation and Digitalization under the Romanian National Core Program LAPLAS VII - contract no. 30N/2023.

References

[1] T. Antoni *et al.* [KASCADE], Astropart. Phys. **24**, 1-25 (2005)

[2] W. D. Apel *et al.* [KASCADE Grande], Phys. Rev. Lett. **107**, 171104 (2011)

[3] M. G. Aartsen *et al.* [IceCube], Phys. Rev. D **100**, no.8, 082002 (2019)

[4] R. U. Abbasi *et al.* [Telescope Array], Astrophys. J. **865**, no.1, 74 (2018)

[5] A. Aab *et al.* [Pierre Auger], Phys. Rev. Lett. **125**, no.12, 121106 (2020)

[6] R. U. Abbasi *et al.* [Telescope Array], Astropart. Phys. **80**, 131-140 (2016)

[7] M. Amenomori *et al.* [Tibet AS_γ], Phys. Rev. Lett. **126**, no.14, 141101 (2021)

[8] Z. Cao *et al.* [LHAASO], Nature **594**, no.7861, 33-36 (2021)

[9] R. Conceição, L. Gibilisco, M. Pimenta and B. Tomé, JCAP **10**, 086 (2022)

[10] A. Bakalová, R. Conceição, L. Gibilisco, V. Novotný, M. Pimenta, B. Tomé and J. Vícha, [arXiv:2304.02988 [hep-ph]].

[11] R. Conceicao, P. J. Costa, L. Gibilisco, M. Pimenta and B. Tome, Eur. Phys. J. C **83**, no.10, 932 (2023)

[12] A. Bakalová, R. Conceição, L. Gibilisco, V. Novotný, M. Pimenta, B. Tomé and J. Vícha, PoS **ICRC2023**, 964 (2023)

[13] A. Haungs, D. Kang, S. Schoo, D. Wochele, J. Wochele, W. D. Apel, J. C. Arteaga-Velázquez, K. Bekk, M. Bertaina and J. Blümer, *et al.* Eur. Phys. J. C **78**, no.9, 741 (2018)

[14] N. Arsene, JCAP **09**, 020 (2023)

[15] T. Antoni *et al.* [KASCADE], Astropart. Phys. **24**, 1-25 (2005)

[16] K. Rawlins [IceCube], J. Phys. Conf. Ser. **718**, no.5, 052033 (2016)

[17] T. K. Gaisser, Astropart. Phys. **35**, 801-806 (2012)

[18] T. K. Gaisser, T. Stanev and S. Tilav, Front. Phys. (Beijing) **8**, 748-758 (2013)

[19] H. P. Dembinski, R. Engel, A. Fedynitch, T. Gaisser, F. Riehn and T. Stanev, PoS **ICRC2017**, 533 (2018)

[20] R. Plaga, New Astron. **7**, 317-336 (2002)

[21] S.P. Swordy, *Proc. 24th Int. Cosmic Ray Conf.*, Rome 2, 697 (1995).

[22] L. G. Sveshnikova, Astron. Astrophys. **409**, 799-808 (2003)